

Can fog contribute to the nutrition of *Chamaecyparis obtusa* var. *formosana*? Uptake of a fog solute tracer into foliage and transport to roots

I-LING LAI,¹ WALTER H. SCHROEDER,^{2,3} JIUNN-TZONG WU,^{1,4} LING-LONG KUO-HUANG,¹ CAROLA MOHL² and CHANG-HUNG CHOU⁵

¹ Institute of Ecology and Evolutionary Biology, National Taiwan University, Taipei 106, Taiwan

² Phytosphere Institute, ICGHI, Research Center Jülich, 52425 Jülich, Germany

³ Corresponding author (w.schroeder@fz-juelich.de)

⁴ Research Center for Biodiversity and Institute of Botany, Academia Sinica, Taipei 115, Taiwan

⁵ Research Center for Biodiversity, China Medical University, 91, Hseuh-Shih Rd., Taichung 404, Taiwan

Received February 24, 2006; accepted November 6, 2006; published online April 2, 2007

Summary Yellow cypress (*Chamaecyparis obtusa* (Siebold & Zucc.) Endl. var. *formosana* (Hayata) Rehder) is the predominant tree species of Taiwan's nutrient-poor, mountain fog forests. Little is known about the potential contribution of solute uptake from fog to the overall nutrition of these trees. Shoots of yellow cypress seedlings were misted with artificial fog containing the tracer rubidium (Rb) in laboratory and field experiments to determine if there is solute uptake from the fog. After misting shoots for six weeks, substantial amounts of tracer were detected in unexposed roots by inductively coupled plasma mass spectroscopy bulk analysis.

Possible routes of entry were examined by element imaging with energy dispersive X-ray analysis. Direct uptake of the tracer into leaves across the cuticle and epidermis was small, excluding this as the major uptake path. Accumulations of Rb were found on leaf surfaces along the edges of the leaves. The almost daily changes in fog coverage and air humidity may enhance the accumulation of fog solutes at leaf edges. Accumulation of Rb was also found in narrow clefts between opposite leaves and between the outermost and underlying alternating stacked leaves. The clefts provide a direct passage from the leaf surface to the space beneath the imbricate leaves and the underlying alternate leaves, possibly facilitating solute uptake from fog, which in turn may contribute to the nutrition of yellow cypress.

Keywords: EDXA, ICP-MS, nutrient-poor forest, rubidium.

Introduction

The effects of long-lasting occurrences of heavy fog on local ecosystems have been investigated, particularly in coastal regions (Hamilton et al. 1994, Weathers 1999, Foster 2001). In some ecosystems, fog provides an important source of water

(Ingraham and Matthews 1995, Dawson 1998), especially in regions where rainfall is scarce during parts of the year.

In addition to water, fog provides an influx of a variety of solutes (e.g., Fuzzi et al. 2002). Depending on the particular ecosystem, both a large variety and quantity of solutes may be transported by fog (e.g., Thalmann et al. 2002, Lange et al. 2003). Several studies of air pollution have demonstrated that some of the most pronounced effects of fog are linked to fog-mediated pollution as a result of “fog-combing” or “cloud-combing” on hillsides, with major detrimental effects to trees (e.g., Dollard et al. 1983, Minami and Ishizaka 1996). At polluted sites, pollutants present at high concentrations are taken up directly by foliage; however, it is not known if trees in unpolluted ecosystems take up naturally occurring solutes carried in fog. Although the relevance of this input is largely unknown, we hypothesized that, besides modulations of biologically relevant physical parameters (e.g., water import, relative humidity, temperature and sunlight), fog-borne nutrient input has a positive effect on the net primary productivity of ecosystems.

At the single plant level, we lack a thorough understanding of fog-mediated solute uptake and the underlying physiological and biophysical mechanisms. Burgess and Dawson (2004) studied the effect of fog on the water relations of a single species and demonstrated that fog could significantly reduce water loss by transpiration and increase foliar water content by up to 6%.

In this study, we investigated uptake of fog-borne solutes by foliage at the single-tree level and the possible routes of entry. We selected *Chamaecyparis obtusa* (Siebold & Zucc.) Endl. var. *formosana* (Hayata) Rehder (yellow cypress) (Li and Keng 1994) for this study because it is the only species that forms pure natural forest canopies in zones of extreme fog in Taiwan (Su 1984).

The Yuanyang Lake Nature Reserve site (YYL), located in the extremely humid, subalpine, mountain fog forests in north-east Taiwan (Liao et al. 2003) include pure stands of yellow cypress that are shrouded by heavy fog for 4–16 h per day (Hwang et al. 1996, Chang et al. 2002). In a previous study at the YYL (Chang et al. 2002), fog-mediated ecosystem inputs of water and solutes were monitored. The fog at the YYL has a high ion content and accounts for more than 50% of total ecosystem ion uptake, whereas it accounted for only 10% of ecosystem water influx. The high total ion input and solute concentrations led us to question whether the dominant plant species utilize this possible source of nutrition.

To determine if fog-mediated solute uptake by foliage occurs, we applied pulses of artificial mist containing the tracer rubidium (Rb) to shoots of yellow cypress seedlings under controlled conditions in growth chambers. Rubidium is a non-toxic tracer that occurs naturally only in low concentrations; in aqueous solution, it behaves similarly to other monovalent ions, particularly potassium. Our specific objectives were to: (1) detect and quantify solute uptake and subsequent transport from shoots to roots by studying the presence of Rb in bulk samples from roots of plants treated with artificial mist containing Rb tracer; and (2) examine possible routes of fog-mediated ion uptake into foliage by microbeam element imaging analysis of foliage of trees exposed to mist containing Rb tracer in growth chambers and at the YYL.

Materials and methods

Site description

The YYL is located at an elevation of 1650–2432 m a.s.l. in a remote area in I-Lan County in northeastern Taiwan (24°35' N, 121°24' E). Although this site is less than 100 km from the heavily industrialized western part of Taiwan, air pollutants do not seem to be transported across the mountain range on the west side of the site. Similarly, the Fu-Shan research site, located 30 km to the northeast of YYL, has relatively low SO_4^{2-} and NO_3^- concentrations in the bulk precipitation.

Yellow cypress dominates the forest, which has an open canopy structure with 850 yellow cypress ha^{-1} . Stand age is 100 years. Fallen trunks are important substrates for the regeneration of yellow cypress. The YYL composition, population structure, growing substrates and recruitment of yellow cypress have been documented in detail by Liao et al. (2003). Heavy moisture results in abundant growth of mosses on the forest floor, tree trunks and fallen logs. Mean annual air temperature is 13 °C; the highest monthly mean is 18 °C in June, and the lowest temperature is 5 °C in January (Hwang et al. 1996). The soils are either partial podzols or nearly pure peat soils with a highly organic surface layer, generally very shallow (< 60 cm) to bedrock and strongly acidic with low mineral nutrient contents (Chiu et al. 1999a, 1999b). Mean annual precipitation at YYL can reach 3400 mm, with a large fraction occurring in occasional heavy rain events, e.g., during typhoons, which contribute 36% of total precipitation. There was an av-

erage of 342 days of dense fog per year in 1994–2004 (Lai et al. 2006).

Seedlings for growth chamber experiments

Yellow cypress seedlings, raised from seed collected in the YYL, were grown in a nursery located near the YYL. Three-year-old seedlings, 30–50 cm in height, were lifted, washed with deionized water and replanted in washed sand in a growth chamber (14-h photoperiod, $100 \mu\text{mol m}^{-2} \text{s}^{-1}$ photosynthetic photon flux (PPF), day/night temperature of 20/15 °C and 85% relative humidity). The growth chamber irradiance corresponds with that measured below the canopy where natural regeneration of yellow cypress is generally found (Lai et al. 2005). Experiments were performed with seedlings acclimated to the growth chamber environment for two months and bearing newly flushed shoots.

Tracer application

Tracer solutions were applied with an artist's airbrush as a nebulizer (Aero-pro 281, 0.2 mm orifice, Hansa, Germany). Drop sizes of the aerosol in the cone of the airbrush were 1–3 μm or less, as crudely determined by spraying onto a cold metal mirror and measuring the size of the frozen droplets by low-temperature scanning electron microscopy (SEM). Selected branches or entire shoots of yellow cypress seedlings were misted in pulses with the indicated concentrations of rubidium chloride (RbCl) in deionized water. Pulses of tracer were applied by misting leaves daily (at 0900 and 1700 h) until they were fully wetted. Plants misted with deionized water served as controls. The plant pot and all but the treated part of the plant were protected from the mist and runoff with polyethylene film (transparent for branches, opaque for pots). Where treated branches emerged through the protective film, a dental cast (Xantopren VL plus, Heraeus Kulzer, Germany) was applied to seal the film around the branch. The cast polymerized within 2 minutes and formed a waterproof, physiologically inert yet flexible seal. Seals were tested for leaks by the application of fluorescein (Merck) and checking for fluorescence beyond the seal with a UV light.

Tracer experiment I: long-term tracer application in a growth chamber

Entire shoots of ten seedlings per tracer concentration (0.1, 0.2, 0.8 or 1.6 mmol l^{-1} RbCl) were misted daily for 6 weeks in a growth chamber. All seedlings were watered once a week with deionized water applied directly to the sand. One hour after the last tracer application, entire plants were removed from the sand, dried with a hair dryer and stored dry in the presence of silica gel. Three root fractions, FI to FIII, each of ~100 mg dry mass, were collected. Fraction FI was the first fraction of the main root below ground, typically about 1 cm in length. Fraction FII was taken immediately below fraction FI. Fraction FIII was a collection of fine roots, each 2–3 cm in length including the root tips, obtained with the aid of a stereomicroscope. One seedling was used as a control plant.

Inductively coupled plasma mass spectrometry (ICP-MS) of bulk root samples

Root fractions FI to FIII were dried, weighed and ashed for 45 min at 200 °C with suprapure HNO₃ (Merck) in a Mars X microwave digestion system (CEM, U.K.) filled to a volume of 10 ml. Because of the high detection sensitivity of the instrument, aliquots of these samples were diluted tenfold with ultrapure water (MilliQ) to meet the linear range of an Elan 6100 mass spectrometer (Perkin-Elmer SCIEX, Thornhill, ON, Canada). In cases where tenfold dilution was insufficient, additional aliquots of the samples were analyzed after 40-fold dilution. Concentrations were determined twice, and external calibration was conducted both before and after each group of 10 samples. Three certified reference materials (NIST 1575 pine needles, NIST 1572 citrus leaves and GBW 07602 bush branches and leaves, containing rhodium as an added internal standard) were used for accuracy control. For the three reference materials, all analyzed elements were within the certified range of concentrations (e.g., for NIST 1575 pine needles: K $0.37 \pm 0.02\%$, Rb $11.7 \pm 0.1 \mu\text{g g}^{-1}$).

Statistical analysis

Data were analyzed by two-way analysis of variance (ANOVA), with tracer concentration and fractions as the fixed factors. Significance of differences of means was tested by Fisher's Least Significant Difference (LSD) test.

Scanning electron microscopy and energy dispersive X-ray analysis

Tracer on leaf surfaces and in branch cross sections was imaged by energy dispersive X-ray analysis (EDXA) using an INCA system (Oxford Instruments, U.K.) with a 10 mm² SiLi detector, at 15 keV and 30 keV, in combination with a scanning electron microscope (LEO Gemini VP 1550, Carl Zeiss, Oberkochen, Germany). Samples were mounted on carbon pads and carbon coated (3.0 nm) by electron beam carbon evaporation (MED 020, BAL-TEC, Germany). Rubidium was identified by the characteristic K α line at 13.40 keV and the Rb-L line at 1.70 keV. The Rb-L line is of higher intensity and was selected for imaging. A possible partial overlap with the Si-K α line at 1.74 keV was excluded by quantitative analysis of pooled spectra of the regions containing Rb. Rubidium mapping required 24–48 hours of instrument time per sample area. For non-imaging measurements of Rb, we defined regions of interest (ROIs) in SEM images (see Figure 3a). The X-ray data in these ROIs were pooled, which shortened the times for data collection (typically 30 min). To determine the detection limit for these conditions, we used the reference material NIST 1575 pine needles. This material is certified at $11.7 \pm 0.1 \mu\text{g g}^{-1}$ Rb. We were able to detect Rb in these samples and extrapolated the detection limit to $5 \mu\text{g g}^{-1}$ Rb. Rubidium could not be detected in the yellow cypress samples or in the two other reference materials, which had certified concentrations of $4.8 \mu\text{g g}^{-1}$ and $4.2 \mu\text{g g}^{-1}$ Rb (although Rb was detectable in these reference materials when analyzed by ICP-MS, see above).

Tracer experiment II: short-term high concentration tracer application in a growth chamber

Branches of growth-chamber seedlings were pulse misted for three days with 10.0 mmol l^{-1} RbCl tracer solutions. To allow direct comparison of the results, we had to use the same specimen preparation protocol in our laboratory and at YYL where provision for shock freezing and cold storage was unavailable. We therefore developed a simplified specimen preparation protocol for use at both the ecosystem study site and in the laboratory. Samples were collected 1 h after the final misting. Branchlet surfaces appeared dry and were further dried with a hair dryer and stored in the presence of silica gel. Another set of misted samples was shock frozen in liquid propane at $-159 \text{ }^\circ\text{C}$ followed by freeze drying at $< -100 \text{ }^\circ\text{C}$. There were no apparent differences in tracer distributions on the leaf surfaces of samples prepared by the simplified preparation protocol and samples that were shock frozen, indicating that major redistribution of Rb did not occur during drying by the simpler protocol. Sixteen branchlets originating from two plants were prepared, and oblique cross sections were analyzed by EDXA to determine the tracer distribution.

Tracer experiment III: short-term high concentration tracer exposure at the YYL site

Six healthy, naturally established, yellow cypress seedlings (height: 30–70 cm) were selected in the YYL in April 2004 for misting on location. Mature branches—the third or fourth branch from the apex—were chosen. The branches were protected against rainfall by a polyethylene film canopy, which was temporarily lifted for tracer application. Pulses of 10 mmol l^{-1} RbCl solution (less than 0.3 ml of total solution) were applied for 2 min to each branch, twice per day on three consecutive days. For sample collection, the target branches were excised 1 h after the final mist application during a dry spell, when leaf surfaces appeared dry. Collected samples were further dried with a hair dryer within 30 min of collection and stored in polyethylene bags with dry silica gel. The distribution of chemical elements, especially K and Rb, within three sections and leaf surfaces of each of the six collected branches were analyzed by EDXA.

Specimen preparation for light microscopy

Samples from branches of yellow cypress collected at YYL were cut to a length of 1 mm. Sections were fixed in 2.5% glutaraldehyde, 2% formaldehyde in 0.1 M phosphate buffer, pH 7.6, post-fixed in 1% OsO₄, dehydrated in an acetone-series and embedded in Spurr's resin (Spurr 1969). Sections of 0.9 μm were cut with an Ultracut E microtome (Reichert-Jung, Vienna, Austria) and stained for light microscopic examination with 0.1% toluidine blue.

Meteorological data

A self-sustained weather station was set up 1 km from the sample site. Photosynthetic photon flux, precipitation, temperature and relative humidity were determined as 5-min means of data taken at 10-s intervals by a quantum sensor (LI-190SZ,

Li-Cor, Lincoln, NE). Rainfall (Takeda Co., Japan) and temperature/relative humidity (HMP35A, Vaisala, Helsinki, Finland) were also recorded. All data were recorded on a data logger (CR10, Campbell Scientific Inc., Logan, UT). The visibility data were recorded at identical intervals with a MIRA visibility sensor (Model 3544, Aanderaa Inst., Norway) in a weather station 3 km from the experiment site.

Results

Rubidium uptake by shoots and transport to roots

To study uptake at the whole-plant level, entire shoots were given daily pulses of tracer applied by misting in a growth chamber for six weeks. In root fractions of control samples, the background concentration of naturally occurring Rb ($0.38 \mu\text{g g}^{-1}$ dry mass) was readily detectable by ICP-MS. Compared with control samples, Rb was detected at significantly higher concentrations in all root fractions of plants whose shoots had been exposed to any concentration of the tracer (Table 1, Figure 1). Because of the close similarity between Rb and K, especially in the hydrated ionic form, we also expressed the tracer concentrations as % of the sum of K and Rb.

There was little difference in tracer concentrations between the first centimeter of the main root (FI) and the adjacent fraction (FII), but the concentration of tracer in fraction FIII, containing root tips, was significantly larger than in fractions FI

Table 1. Concentrations of rubidium (Rb) and potassium (K) in root fractions FI, FII and FIII from the tracer experiment. The concentrations were determined by inductively coupled plasma mass spectrometry analysis. Means and standard deviations (SD) are shown ($n = 10$ except for the 0.2 mmol l^{-1} tracer concentration series where, because of the loss of one plant, $n = 9$). Because of the well established natural Rb concentration, only one seedling was used as a control plant.

Tracer (mmol l^{-1})	FI	SD	FII	SD	FIII	SD
<i>Rb ($\mu\text{mol g}^{-1}$)</i>						
0	0.4	—	0.7	—	0.6	—
0.1	3.1	1.8	3.1	1.9	5.9	3.7
0.2	10.0	6.0	7.1	2.3	19.9	8.4
0.8	34.3	17.1	30.1	9.0	74.6	53.1
1.6	41.1	31.8	31.6	17.8	75.1	35.3
<i>K ($\mu\text{mol g}^{-1}$)</i>						
0	67.3	—	74.9	—	319.0	—
0.1	69.1	10.8	77.7	21.0	225.6	71.7
0.2	70.9	19.3	86.3	18.0	285.2	102.3
0.8	52.2	13.4	70.6	14.3	211.7	95.7
1.6	49.3	13.3	57.3	9.0	215.7	61.2
<i>Rb/(Rb+K)</i>						
0	0.6	—	0.9	—	0.2	—
0.1	4.1	1.8	3.6	1.4	2.7	1.7
0.2	12.5	6.9	7.7	2.4	6.6	2.2
0.8	38.7	7.8	29.9	7.3	25.4	7.5
1.6	41.8	14.8	33.9	11.5	25.1	8.8

and FII. Rubidium concentrations in the root fractions correlated linearly with the tracer concentrations in the misting solutions (0.1 to 0.8 mmol l^{-1}); however, no significant difference was detected in Rb concentrations of root tissues for misting treatments containing between 0.8 and 1.6 mmol l^{-1} of tracer.

Localizing tracer on leaves of growth-chamber plants

Yellow cypress branchlets were flat, with opposite, scale-like, densely imbricate and closely compressed leaves (Figures 2a and 2b; see also Li and Keng 1994). Scanning electron microscopy revealed that the stomata are sunken and situated below Florin rings, which are circular hood-like structures formed by subsidiary cells (Figures 2b and 2c; Florin 1931, Buchholz and Gray 1948, Oladele 1983). Narrow clefts are formed between opposite leaves and in the sandwich between the top and underlying alternating stacked leaves. The Florin rings appeared unevenly distributed and more frequent near the clefts.

On leaf surfaces of control branchlets, the background concentration of naturally occurring Rb was below the detection limit of EDXA. In contrast, large numbers of particles, containing Rb as a major constituent, were detected by EDXA on both abaxial and adaxial leaf surfaces of plants misted with

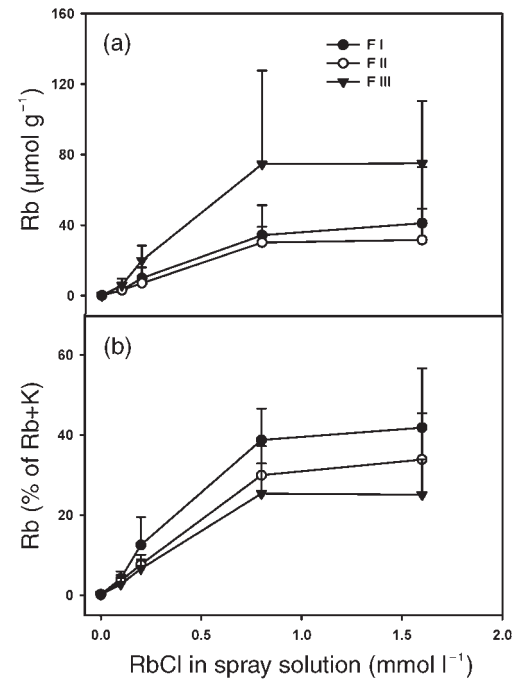


Figure 1. Tracer uptake into root fractions. (a) Rubidium (Rb) concentration in root dry mass and (b) the atom-percentage of Rb in the sum of Rb and potassium (K) in three fractions of yellow cypress root plotted against the tracer concentration in the misting solution. Entire shoots were exposed to the Rb tracer by pulses of mist over a 6-week period in a growth chamber. The root fraction samples were: FI, the first ~100 mg of the main root below ground (typically about 1 cm in length); FII, the subsequent 100 mg fraction; and FIII, fine roots of 2–3 cm length including the root tips ($n = 10$; means + standard deviations).

tracer in experiments I and II (Figure 2c). The concentration of tracer had no obvious effect on the Rb concentration of the particles or on the distribution of particles on leaf surfaces, but the number of larger particles observed in EDXA images increased with Rb tracer concentration. In cases where leaves were sprayed preferentially from one side, the tracer was detected at higher concentrations on the directly exposed surface.

Search for a possible uptake path by imaging rubidium in sections of branchlets

We used 10 mmol l^{-1} Rb and an exposure time of three days

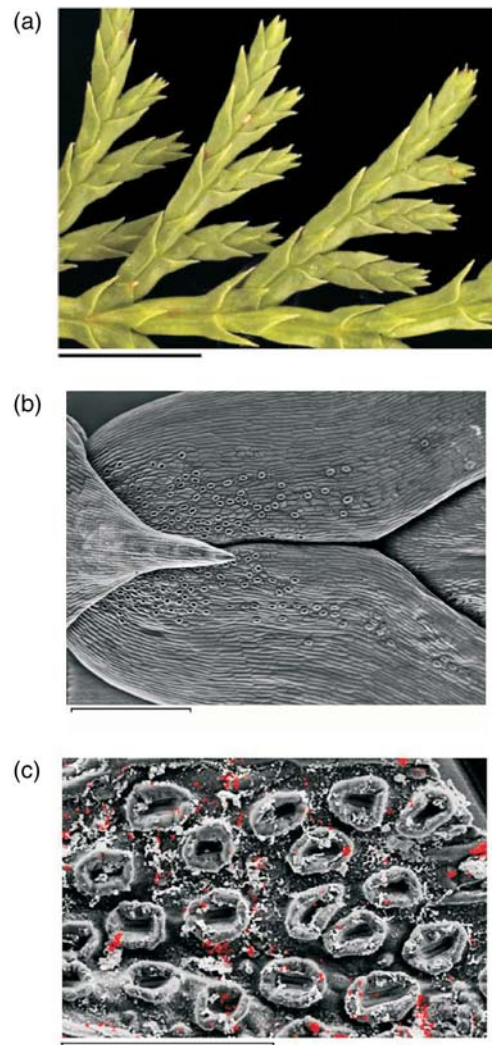


Figure 2. Anatomy of yellow cypress leaves. (a) Yellow cypress branchlets. The scale bar indicates 5 mm. (b) Scanning electron micrograph of abaxial surfaces of native hydrated leaves, without fixation or coating. Florin rings appear more frequently near the cleft formed by the two opposite leaves in the center. The scale bar indicates 500 μm . (c) An area near the edge of a cleft where Florin rings are clustered. The rubidium (Rb) distribution as obtained from energy dispersive X-ray analysis is shown in the red colored overlay. The Rb tracer deposits were observed after 3 days of tracer application with 10 mmol l^{-1} concentration. The scale bar indicates 100 μm .

(tracer experiment II) to image the tracer in internal structures in oblique cross sections of branchlets (Figure 3b). The short exposure time was chosen to minimize diffusion of Rb in the plant tissues. The high concentration of tracer was necessary because of the lower detection sensitivity of EDXA compared with bulk analysis by ICP-MS.

Concentrations of Rb were detected in clefts between adja-

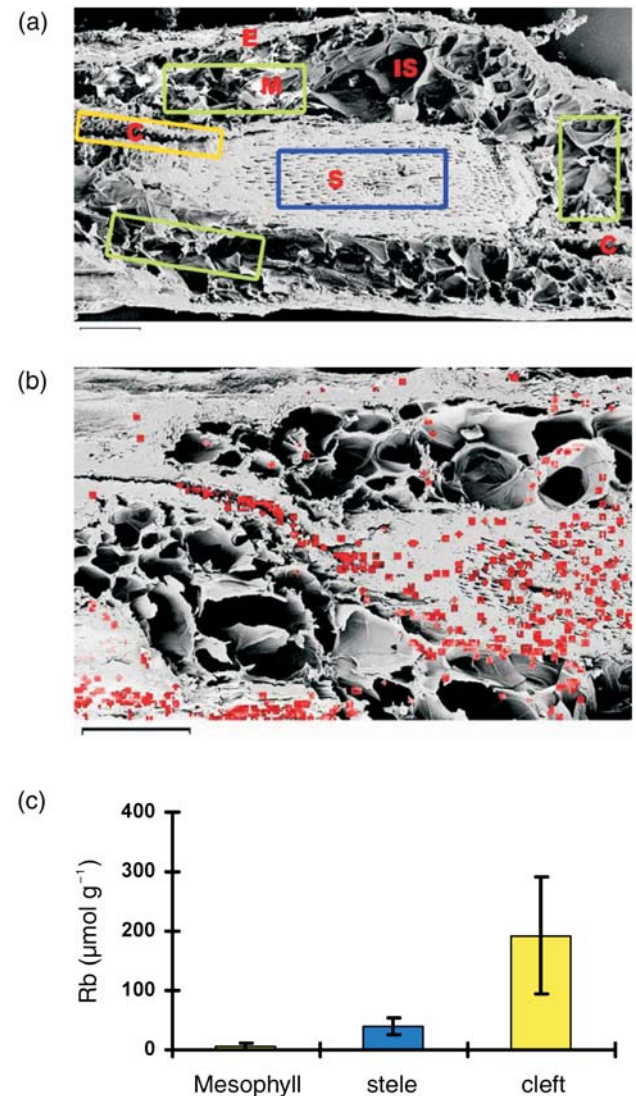


Figure 3. Scanning electron micrographs (SEM) obtained from two oblique cross sections of two yellow cypress branchlets. (a) Scanning electron micrograph of one oblique section. Abbreviations: C, cleft; E, epidermis; IS, intercellular space; M, mesophyll cells; and S, stele. Three regions of interest (ROIs) for element analysis are indicated: blue = stele, yellow = cleft, and green = mesophyll. (b) A tighter cropped SEM of another oblique section. This is overlaid in red with the rubidium (Rb) distribution obtained by energy dispersive X-ray analysis element mapping. The Rb deposits result from tracer applications at 10 mmol l^{-1} after three days. The strong Rb signal at the bottom of the image results from the external epidermal surface. The scale bars represent 200 μm . (c) Rubidium concentrations in the ROIs defined above. Values are means \pm SD; $n = 16$.

cent leaves and in the space between leaves and the stele (Figure 3b). Significant amounts of tracer were also visible in the stele, whereas only small amounts were found in the mesophyll (Figure 3c). A similar pattern of tracer distribution (Figures 3b) was found in all 16 samples examined. Quantification of the tracer was performed by analysis in three defined ROIs (Figures 3a and 3c).

Tracer experiment at YYL

Light microscopy of leaves from plants growing at the YYL revealed that the outer leaf surface was covered with a thick cuticle, an epidermis and a hypodermis (Figure 4). Within the cleft, the cuticle was less pronounced, if present at all, and the hypodermis appeared discontinuous. Stomata and Florin rings were more abundant near and inside the cleft between leaves than on the exposed outer leaf surface. The mesophyll tissue exhibited large intercellular spaces. The cleft between the leaves seemed partially filled with an extracellular matrix of unknown composition. The extracellular matrix material was abundant near the stele (lower right in Figure 4) but was more or less absent near the opening of the cleft.

Localizing Rb on leaves from unexposed plants at YYL

High-magnification SEM of external surfaces of control leaves collected from the YYL revealed epiphytic fungal, bacterial and moss growth, some of which were also evident at low magnification (Figure 5a). Scanning electron microscopy allowed identification of occasional particles on the leaf surfaces that contained various elements, such as Al, Si, K and Ca (deter-

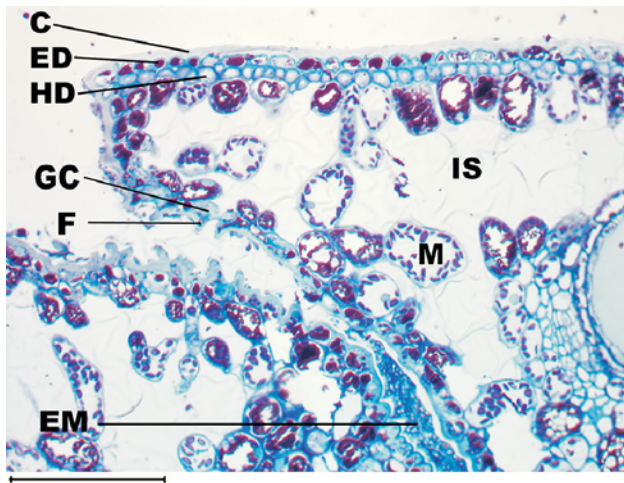


Figure 4. Light micrograph of a cross section of a fixed and resin embedded yellow cypress leaf. Part of two adjacent leaves and the enclosed cleft between the leaves is shown. On the outer leaf surface of the top leaf are the pronounced cuticle (C), the epidermis (ED) and the hypodermis (HD). The hypodermis does not continue into the area of the cleft, and the cuticle appears rudimentary. The sunken stomata with guard cells (GC) and Florin rings (F) appeared clustered in this area. An extracellular matrix (EM) of unknown composition is present in the inner part of the cleft. The mesophyll cells (M) are loosely arranged with ample intercellular space (IS). The scale bar represents 50 μ m.

mined by EDXA; data not shown), but no Rb was detected on control leaf surfaces.

Localizing Rb on leaves from tracer exposed branchlets

After exposure to the tracer, distributions of Rb on the surfaces of leaves collected at the YYL (tracer experiment III) (Figure 5a) differed greatly from patterns observed on leaf surfaces of plants misted in the growth chambers. At the YYL, only a few Rb-containing particles, similar to the ones shown in Figure 2c, were detected except where ridges and clefts were formed by leaf edges. Here, the tracer was localized at high concentrations (Figure 5b). Although we found variation in the absolute amounts of tracer, the distribution pattern shown in Figure 5b was found in all six samples analyzed. On some leaf surfaces, we detected signs of epiphytic growth by SEM (Figure 5a), and most of these epiphytes contained Rb.

Humidity changes at YYL Changes in relative humidity recorded near the experimental site for a typical period in the summer of 2004 are shown in Figure 6. The decrease in visibil-

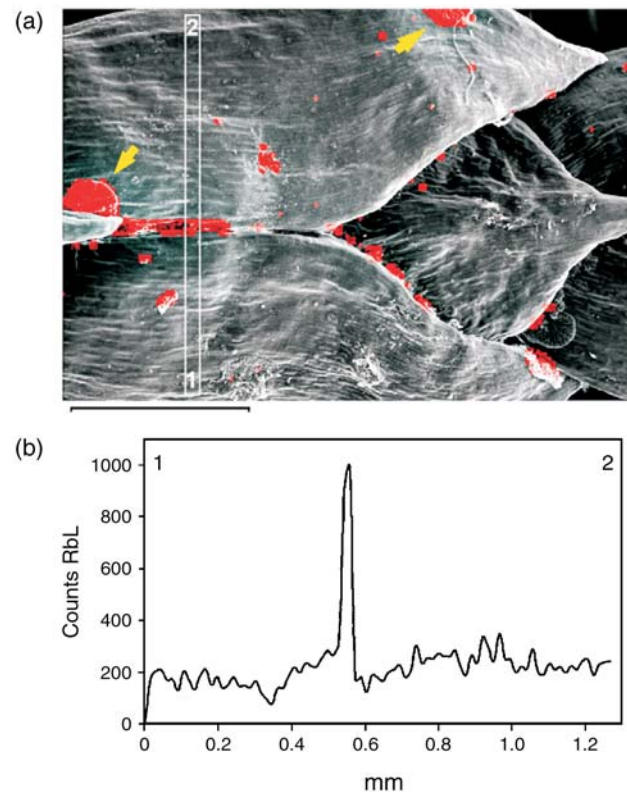


Figure 5. Rubidium (Rb) tracer distribution on the surface of a yellow cypress leaf from the Yuanyang Lake Nature Reserve site (YYL). (a) Image of the Rb tracer distribution on the adaxial surface of a leaf that was misted with tracer while attached to a plant growing at the YYL. The mapping was obtained by overlaying the scanning electron micrograph (SEM) with a red color-coded image representing the Rb detected by EDXA. The arrows point to epiphytic growths containing Rb. The scale bar represents 500 μ m. (b) Linear profile plot of the integrated Rb signal across the boxed region indicated in the SEM in panel a.

ity recorded in Figure 6a indicates the occurrence of dense fog. Fog was mostly associated with supersaturated humidity (see Figure 6b) and typically resulted in visible wet deposition on plant surfaces. However, the concurrence of heavy fog and nominal 100% humidity did not necessarily result in wet precipitation (Figure 6c), defined as precipitation that exceeded the detection limit of 0.5 mm per day. Short periods of reduced humidity were associated with the absence of fog, elevated PPF and at least partial leaf surface drying. These periods of reduced humidity occurred almost daily during the summer months but were less frequent during the rest of the year (data not shown).

Discussion

Rubidium as a tracer

We used Rb as a tracer to monitor uptake of solutes from fog because the physicochemical properties of the hydrated monovalent cations of Rb^+ are similar to those of the macronutrient K^+ (Shannon 1976). Therefore, Rb is not only useful as a general tracer for the ensemble of monovalent cations in local fog, but closely mimics K^+ diffusion, accessibility, uptake and apoplast transport. Transport of Rb^+ across membranes likely differs from K^+ transport and may be slightly less than that of

K^+ (Marschner and Schimansky 1968, Reintanz et al. 2002).

Yellow cypress at YYL

Yellow cypress is the major biomass producer and the exclusive tree species of the mature mountainous fog forests at YYL. In the nutrient-poor and shallow acidic soils at this location, *Chamaecyparis* roots appear poorly developed (Chiu et al. 1999a, 1999b). Light microscopy studies revealed no root hairs or mycorrhizae on roots collected from seedlings growing at the YYL (data not shown), leading us to question if solute uptake from fog by foliage can supplement the poor nutrient supply from the soil.

Fog solutes at YYL

According to a recent study (Chang et al. 2002), fog carries over 50% of the total ion input into the YYL ecosystem (the rest is mainly derived from bulk precipitation). All major ions carried by fog contribute to plant nutrition and are present in fog at roughly 10-fold higher concentrations than in bulk precipitation. Chang et al. (2002) report the most relevant ions for nutrition (median to maximum in $\mu\text{eq l}^{-1}$): Mg^{2+} , 13–67; K^+ , 9–29; Ca^{2+} , 30–229; NH_4^+ , 22–292; and NO_3^- , 28–251). At such high concentrations, ion channels and transporters (see Blatt 1985) could result in substantial foliar nutrient uptake from fog.

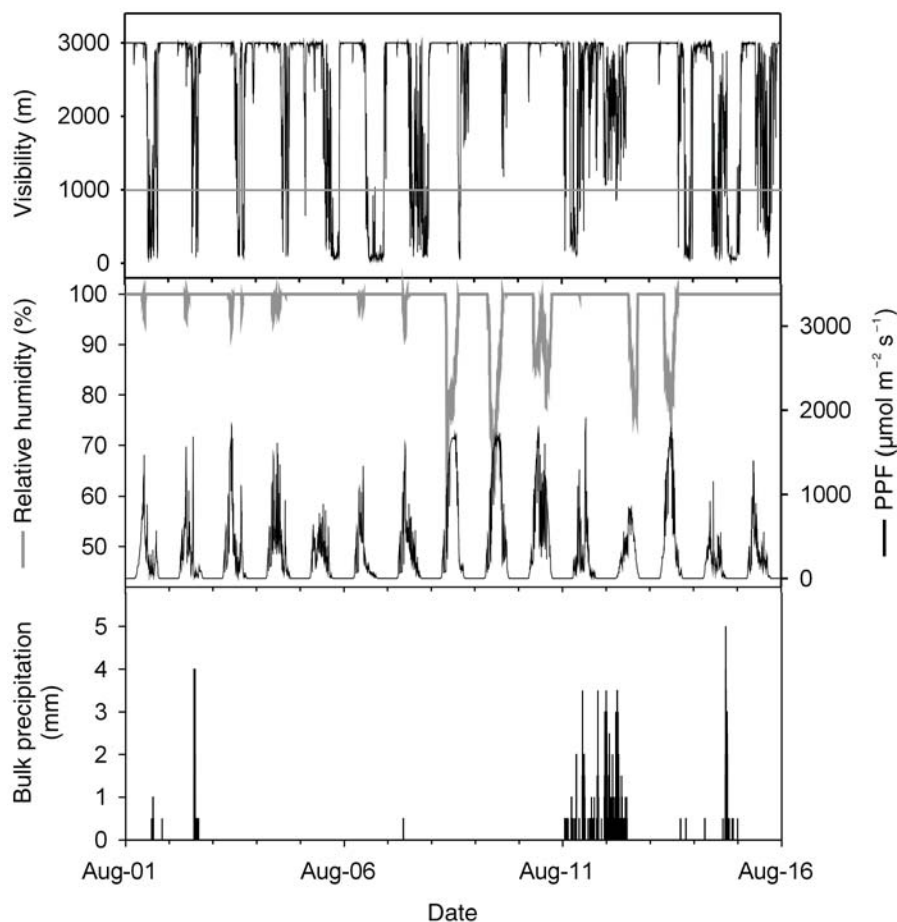


Figure 6. Diurnal changes in weather conditions at the Yuanyang Lake Nature Reserve site from August 1 to 15, 2004: (a) visibility (the solid line at a visibility of 1000 m is the defined borderline of fog occurrence); (b) relative humidity (upper curve) and photosynthetic photon flux (PPF; lower curve); and (c) bulk precipitation plotted in 0.5 mm steps for each day.

Naturally occurring uptake of nutrients by foliage has rarely been reported, despite its potential importance to nutrient cycling within ecosystems. In agriculture, foliar nutrition has been well studied because of its convenience as a method of fertilizer application. However, uptake of leaf applied nutrients typically requires a surfactant (Taiz and Zeiger 1998) or carrier to permeate the hydrophobic, diffusion-limiting cuticle and the hypodermis. The passage of wet deposited solutes across stomata is generally considered to be slight (e.g., Schönherr and Bukovac 1972, Eichert et al. 1998). This is in contrast to the case of pollutants (e.g., Wilson and Tiley 1998), where uptake of wet and dry depositions have been reported, usually because of cuticular or stomatal damage. Thus, the mechanisms responsible for foliar uptake of pollutants appear to differ from those of naturally occurring solutes.

Shoot Rb uptake and tracer transport into roots

We observed significant uptake and subsequent transport of Rb to roots after six weeks of 0.1 mmol l⁻¹ Rb tracer application. This is a lower concentration than the total concentration of monovalent cations and lower than the peak concentrations for some individual ion species found in YYL fog. Tracer uptake appeared to be concentration-dependent, being roughly linearly related to a tracer concentration of up to 0.8 mmol l⁻¹, with an indication of saturation at 1.6 mmol l⁻¹. Within the tracer concentration range of 0.1 to 0.8 mmol l⁻¹, we found Rb in the roots ranging from 3.5 to 30% of the total Rb + K pool (Figure 1), indicating a remarkably high potential to supplement nutrition in yellow cypress by foliar uptake. In agreement with root growth, the root fraction containing the root tips (FIII) contained the highest K concentration as well as the highest Rb concentration.

We used tracer concentrations ranging from 0.1 to 1.6 mmol l⁻¹, and the highest concentrations were at least one order of magnitude higher than the sum of maximal cation concentrations required for adequate nutrition. These high Rb concentrations were applied to determine the maximum capability of foliar uptake and to facilitate imaging of the routes of entry. Further studies are required for any extrapolation to natural conditions, to longer time scales, to cations other than K⁺ and to anions.

The leaves of yellow cypress seem well protected against leaf water loss and solute exchange by thick layers of cuticular wax and cutin, hypodermis and sunken stomata. Light microscopy and SEM of exposed leaf outer surfaces show a well-developed cuticle and epidermis without evidence of wounding or damage. The particular structure and distribution of the stomata have been interpreted as adaptations to minimize water loss (Florin 1931, Zobel et al. 1978) and seems to prevent solute uptake. In agreement with this, we found no evidence of transport occurring across the leaf cuticle or via the stomata. In surface views (Figure 2c) and in cross sections (Figure 3b lower left) of leaves from misted branches, we found large accumulations of tracer on the external exposed surfaces of leaves. Tracer was also present in the clefts formed between leaves and in the space between leaves and the stele (Figure 3).

In the same cross sections, we also detected tracer in the stele. Only negligible amounts of tracer were detected in the mesophyll. If the tracer reached the stele across the leaves, then larger amounts of tracer should have been detected in the mesophyll.

Our findings support the following model. Water and solutes are deposited on leaves during fog exposure (Chang et al. 2002). Together with the fog water, solutes may be taken up. When the relative humidity is reduced, the water film on leaf surfaces evaporates. The hydrophobic properties of the outer leaf surfaces force the surface water toward the leaf edges, especially near clefts, where the edges of the two opposite leaves meet (Figures 2b and 5a). The narrow clefts continue to the underlying leaves and stem. Residual surface-water can be drawn into these underlying clefts by capillary forces, and solutes equilibrate between the outer surface and the extracellular space in the clefts. With increasing evaporation during dry spells, the local concentrations of solutes increase and the resulting increased concentration gradient can facilitate solute uptake. Repeated cycles of surface drying and wetting further enhance this effect. The highest concentrations of solutes occurred near and in the clefts where they would be most available for absorption. Thus, an efficient nutrient uptake mechanism is inherent in the simple branchlet of yellow cypress.

The finding that the leaf surfaces facing the clefts lack a hypodermis and a visible cuticle led us to speculate that this may be a preferential site for uptake into mesophyll cells. Although we found no evidence of major uptake of Rb⁺ into the mesophyll, this may be a preferential site of uptake of ions other than our tracer, perhaps anions or ions requiring carriers for transport. Given the timescale of our experiments, any incoming tracer would have mixed with the K⁺ originally present in the cell, and this would result in a large change in the Rb/K ratio. Because a change in this ratio was not observed, we conclude that transport across the mesophyll is of minor importance and that a direct apoplastic passage between the two areas with highest tracer concentrations, the cleft and the stele, is the most likely route for foliar uptake of fog-borne solutes.

Acknowledgments

The authors acknowledge the use of the SEM facilities of the Institut für Schichten und Grenzflächen (ISG) at the Forschungszentrum Jülich. Travel expenses were covered by grants obtained by a Project-based Personnel Exchange Program (PPP-project) from Deutscher Akademischer Austauschdienst (DAAD) and the National Science Council (NSC) of Taiwan given to W. H. Schroeder and J. T. Wu. We are grateful to Forest Protection Department under The Veterans Affairs Commission of the Executive Yuan of the Republic of China for the supply of seedlings. The visibility data of Figure 6 were kindly provided as a courtesy by Dr. S. C. Chang, Dong-Hwa University. We thank B. Uhlig, M. Roeb and M Müller for technical help and B. Buchen, A. Kuhn, H. Lühring, P. Minchin and V. Temperton for critical reading of the manuscript.

References

- Blatt, M.R. 1985. Extracellular potassium activity in attached leaves and its relation to stomatal function. *J. Exp. Bot.* 36:240–251.

- Buchholz, J.Z. and N.E. Gray. 1948. A taxonomic revision of *Podocarpus*. I. The sections of the genus and their subdivisions with special reference to leaf anatomy. *J. Arnold Arbor. Harvard Univ.* 29:49–63.
- Burgess, S.S.O. and T.E. Dawson. 2004. The contribution of fog to the water relations of *Sequoia sempervirens* (D. Don): foliar uptake and prevention of dehydration. *Plant Cell Environ.* 27:1023–1034.
- Chang, S.C., I-L. Lai and J.T. Wu. 2002. Estimation of fog deposition on epiphytic bryophytes in a subtropical montane forest ecosystem in northeastern Taiwan. *Atmos. Res.* 64:159–167.
- Chiu, C.Y., S.Y. Lai, Y.M. Lin and H.C. Chiang. 1999a. Distribution of the radionuclide ¹³⁷Cs in the soils of a wet mountainous forest in Taiwan. *Appl. Radiat. Isot.* 50:1097–1103.
- Chiu, C.Y., S.Y. Lai, C.J. Wang and Y.M. Lin. 1999b. Transfer of ¹³⁷Cs from soil to plants in a wet montane forest in subtropical Taiwan. *J. Radioanal. Nucl. Chem.* 239:511–515.
- Dawson, T.E. 1998. Fog in the California redwood forest: ecosystem inputs and use by plants. *Oecologia* 117:476–485.
- Dollard, G.J., M.H. Unsworth and M.J. Harve. 1983. Pollutant transfer in upland regions by occult precipitation. *Nature* 302:241–243.
- Eichert, T., H.E. Goldbach and J. Burkhardt. 1998. Evidence for the uptake of large anions through stomatal pores. *Bot. Acta* 111:461–466.
- Florin, R. 1931. Untersuchungen zur Stammesgeschichte der Coniferales und Cordaitales. Erster Teil: Morphologie und Epidermisstruktur der Assimilationsorgane bei den rezenten Koniferen. *Kung. Svenska Vetenskapsakademiens Handlingar*, n.s. 3, Band 10. Almqvist & Winstells Boktryckeri, Stockholm, 588 p.
- Foster, P. 2001. The potential negative impacts of global climate change on tropical montane cloud forests. *Earth-Sci. Rev.* 55:73–106.
- Fuzzi, S., M.C. Facchini, E.M. Decesari and M. Mircea. 2002. Soluble organic compounds in fog and cloud droplets: what have we learned over the past few years? *Atmos. Res.* 64:89–98.
- Goldsmith, J.G., D.B. Lazof, W.H. Schroeder, A.J. Kuhn, T.W. Ruffy and R.W. Linton. 1994. SIMS ion image analysis for quantification of isotope labels and nutrient tracers in plant tissues. *In Proc. Ninth International Conference on Secondary Ion Mass Spectrometry*. Eds. A. Benninghoven, Y. Nihei, R. Shimizu and H.W. Werner. John Wiley and Sons, Hoboken, pp 824–827.
- Hamilton, L.S., J.O. Juvik and F.N. Scatena. 1994. The Puerto Rico tropical cloud forest symposium: introduction and workshop synthesis. *In Tropical Montane Cloud Forests*. Eds L.S. Hamilton, J.O. Juvik and F.N. Scatena. Springer-Verlag, New York, pp 1–23.
- Hwang, Y.H., C.W. Fang and M.H. Yin. 1996. Primary production and chemical composition of emergent aquatic macrophytes, *Schoenoplectus mucronatus* ssp. *robustus* and *Sphagnum fallax*, in Lake Yuan-yang, Taiwan. *Bot. Bul. Acad. Sin.* 37:265–273.
- Ingraham, N.L. and R.A. Matthews. 1995. The importance of fog-drip to vegetation: Point Reyes Peninsular, California. *J. Hydrol.* 164:269–285.
- Lai, I-L., H. Scharr, A. Chavarria-Krauser, R. Küsters, J.-T. Wu, C.-H. Chou, U. Schurr and A. Walter. 2005. Leaf growth dynamics of two congener gymnosperm tree species reflect the heterogeneity of light intensities given in their natural ecological niche. *Plant Cell Environ.* 28:1496–1505.
- Lai, I-L., S.-C. Chang, P.-H. Lin, C.-H. Chou and J.-T. Wu. 2006. Climate characteristics of the subtropical mountainous cloud forest at the Yuanyang Lake long-term ecological research site, Taiwan. *Taiwania* 51:317–329.
- Lange, C.A., J. Matschullat, F. Zimmermann, G. Sterzik and O. Wienhaus. 2003. Fog frequency and chemical composition of fog water – a relevant contribution to atmospheric deposition in the eastern Erzgebirge, Germany. *Atmos. Res.* 37:3731–3739.
- Li, H.L. and H. Keng. 1994. Cupressaceae. *In Flora of Taiwan*. 2nd Edn. Dept. Botany, National Taiwan University, Taipei, Vol. 1, pp 586–595.
- Liao, C.C., C.H. Chou and J.T. Wu. 2003. Population Structure and Substrates of Taiwan yellow false cypress (*Chamaecyparis obtuse* var. *formosana*) in Yuanyang Lake Nature Reserve and nearby Szumakuszu, Taiwan. *Taiwania* 48:6–21.
- Marschner, H. and C. Schimansky. 1968. Differential uptake of potassium and rubidium by barley. *Naturwissenschaften* 55:499–503.
- Minami, Y. and Y. Ishizaka. 1996. Evaluation of chemical composition in fog water near the summit of a high mountain in Japan. *Atmos. Environ.* 30:3363–3376.
- Oladele, F.A. 1983. Scanning electron microscope study of stomatal-complex configuration in Cupressaceae. *Can. J. Bot.* 61:1232–1240.
- Reintanz, B., A. Szyroki, N. Ivashikina, P. Ache, M. Godde, D. Becker, K. Palme and R. Hedrich. 2002. AtKC1, a silent *Arabidopsis* potassium channel α -subunit modulates root hair K⁺ influx. *Proc. Natl. Acad. Sci. USA* 99:4079–4084.
- Schönherr, J. and M.J. Bukovac. 1972. Penetration of stomata by liquids. Dependence on surface tension, wettability, and stomatal morphology. *Plant Physiol.* 49:813–819.
- Shannon, R.D. 1976. Revised effective ionic radii in halides and chalcogenides. *Acta Crystallogr.* 32:751–767.
- Spurr, A.R. 1969. A low-viscosity epoxy resin embedding medium for electron microscopy. *J. Ultrastruct. Res.* 26:31–43.
- Su, H.J. 1984. Studies on the climate and vegetation types of the natural forests in Taiwan. II. Altitudinal vegetation zones in relation to temperature gradient. *Quart. J. Chin. For.* 17:57–73.
- Taiz, L. and E. Zeiger. 1998. Mineral nutrition. *In Plant Physiology*. 2nd Edn. Sinauer Associates, Inc. Sunderland, MA, pp 103–124.
- Thalmann, E., Burkard R., Wrzesinsky T., Eugster W. and O. Klemm. 2002. Ion fluxes from fog and rain to an agricultural and a forest ecosystem in Europe. *Atmos. Res.* 64:147–158.
- Weathers, K.C. 1999. The importance of cloud and fog in the maintenance of ecosystems. *Trends Ecol. Evol.* 14:214–215.
- Wilson, E.J. and C. Tiley. 1998. Foliar uptake of wet-deposited nitrogen by Norway spruce: an experiment using ¹⁵N. *Atmos. Environ.* 32:513–518.
- Zobel, D.B., T.P. Lin and V.T. Liu. 1978. Stomatal distribution on leaves of three species of *Chamaecyparis*. *Taiwania* 23:1–6.